Spronck, B.; Latorre, M.; Wang, M.; Mehta, S.; Caulk, AW.; Ren, P.; Ramachandra, AB.... (2021). Excessive adventitial stress drives inflammation-mediated fibrosis in hypertensive aortic remodelling in mice. Journal of The Royal Society Interface. 18(180):1-11. https://doi.org/10.1098/rsif.2021.0336

Excessive Adventitial Stress Drives Inflammation-Mediated Fibrosis in Hypertensive Aortic Remodeling in Mice

Bart Spronck[1,2], Marcos Latorre[1], Mo Wang[3], Sameet Mehta[4], Alexander W. Caulk[1], Pengwei Ren[3], Abhay B. Ramachandra[1], Sae-Il Murtada[1], Alexia Rojas[1], Chang-Shun He[3], Bo Jiang[3], Matthew R. Bersi[5], George Tellides[3,6], Jay D. Humphrey[1,6]

[1]Department of Biomedical Engineering
Yale University, New Haven, CT, USA

[2]Department of Biomedical Engineering
Maastricht University, Maastricht, Netherlands

[3]Departments of Surgery and [4]Genetics
Yale School of Medicine, New Haven, CT, USA

[5]Department of Mechanical Engineering and Materials Science
Washington University in St. Louis, St. Louis, MO, USA

[6]Vascular Biology and Therapeutics Program
Yale School of Medicine, New Haven, CT, USA

Short title:	*Immuno-mechanics in aortic remodeling*
Manuscript body word-count:	6747
Abstract word-count:	200
Figures/tables/supplements:	5/0/5

Correspondence:
B. Spronck, Ph.D.
Department of Biomedical Engineering
Maastricht University, Maastricht, Netherlands
b.spronck@maastrichtuniversity.nl

or,

J.D. Humphrey, Ph.D.
Department of Biomedical Engineering
Yale University, New Haven, USA
jay.humphrey@yale.edu

Abstract

Hypertension induces significant aortic remodeling, often adaptive but sometimes not. To identify biomechanical mechanisms responsible for differential remodeling, we studied thoracic aortas from 129S6/SvEvTac and C57BL/6J mice before and after continuous 14-day angiotensin II infusion, which elevated blood pressure similarly in both strains. Histological and biomechanical assessments of excised vessels were similar at baseline, suggesting a common homeostatic set-point for wall stress. Histology further revealed near mechano-adaptive remodeling of the hypertensive 129S6/SvEvTac aortas, but grossly maladaptive remodeling of the C57BL/6J aortas. Bulk RNA sequencing suggested that increased smooth muscle contractile processes promoted mechano-adaptation in 129S6/SvEvTac aortas while immune processes prevented adaptation of C57BL/6J aortas. Functional studies confirmed an increased vasoconstrictive capacity of the former while immunohistochemistry demonstrated marked increases in inflammation in the latter. We then used three different computational biomechanical models to test the hypothesis that excessive adventitial wall stress correlates with inflammatory cell infiltration. These models consistently predicted that increased vasoconstriction against an increased pressure coupled with modest deposition of new matrix thickened the wall appropriately, restoring wall stress toward homeostatic consistent with adaptive remodeling. In contrast, insufficient vasoconstriction permitted high wall stresses and exuberant inflammation-driven matrix deposition, especially in the adventitia, reflecting compromised homeostasis and gross maladaptation.

Keywords: aorta, fibrosis, stiffness, inflammation, contractility, C57BL/6J, 129S6/SvEvTac, smooth muscle phenotype

Introduction

Homeostasis is a ubiquitous biological process by which certain key regulated variables are maintained near target values, often called set-points.[1] The literature is replete with reports that flow-induced wall shear stress and pressure-induced intramural stress tend to be maintained near individual set-points in the aorta, thus revealing a mechanical homeostasis at the tissue level.[2-5] In cases of preserved blood flow but sustained elevations of blood pressure, homeostatic restorations of intramural stress require the wall to thicken proportional to the fold-increase in blood pressure.[6] Notwithstanding many reports of such homeostatic mechano-adaptations, there are also reports wherein wall thickening is excessive, often fibrotic, thus reflecting a compromised homeostasis.[7,8] It has been shown further that infiltrating inflammatory cells play key roles in these cases of fibrotic aortic remodeling,[9,10] yet it remains unclear what drives the excessive inflammatory response. Indeed, inflammation is essential for promoting a homeostatic adaptation in other cases of altered hemodynamics in central arteries.[11,12]

The goal of this work, therefore, is to understand better the biomechanical mechanisms that either promote or prevent homeostatic aortic remodeling in hypertension. Our specific approach is motivated by two critical observations. First, hypertension induced by chronic infusion of angiotensin II (AngII) at a moderate rate (490 ng/kg/min) causes an inflammation-mediated fibrotic remodeling of the thoracic aorta in C57BL/6[9] but not C57BL/6;129S6/SvEvTac mice.[13] Second, although it may be natural to conjecture that these differences are due mainly to genetic background, the thoracic aorta but not the infrarenal abdominal aorta experiences fibrotic remodeling in high rate (1000 ng/kg/min) AngII-infused *Apoe*$^{-/-}$ mice on a pure C57BL/6 background.[14] It is thus more than genetic background and more than just the rate of infusion of a pro-inflammatory substance (AngII) used to induce the hypertension. In this work, we use consistent methods to contrast directly the gene expression, composition, properties, and function of thoracic aortas from pure C57BL/6J and 129S6/SvEvTac mice before and after two weeks of chronic AngII infusion to uncover biomechanical mechanisms that drive hypertensive aortic remodeling.

Methods

This section provides a brief summary of the methods employed. For details, please refer to Supplemental Digital Content 1.

Animals. Adult mice were obtained from Jackson Laboratory and Taconic Biosciences. Blood pressure was measured using a standard tail-cuff before and after infusion of AngII at 1000 ng/kg/min for two weeks using subcutaneous osmotic mini-pumps. The two-week infusion duration was based on a previous observation that AngII-induced hypertensive remodeling tends not to differ over two-to-four

weeks of infusion.[15,16] Following euthanasia, four groups of descending thoracic aortas were harvested for study (n=5–8 per group): normotensive (control) and hypertensive (AngII-infused) C57BL/6J and 129S6/SvEvTac. All animal protocols were approved by the Yale University IACUC and conformed with Federal guidelines.

Experiments on excised aortas. Aortas were mounted between glass micropipettes, pressurized, and subjected to a series of contraction/relaxation protocols to KCl, AngII, phenylephrine, acetylcholine, and N_{ω}-Nitro-L-arginine methyl ester (L-NAME). Vessels were then preconditioned and exposed to a passive biaxial testing protocol including three inflation cycles at increasing levels of axial stretch, and four extension cycles at increasing levels of pressure. Formalin-fixed sections of the tested vessels were stained for collagen, elastin, smooth muscle, and ground substance. Resulting images were used to quantify mass fractions of said constituents. A separate set of aortas was snap frozen directly after excision and used for next-generation bulk RNA sequencing, yielding differentially expressed genes, -gene ontologies, and -pathways between groups.

Computational modeling. Three different computational biomechanical modeling approaches were used to describe and interpret the acquired biaxial biomechanical testing data. First, a thin-walled, uni-layered model was used incorporating a neo-Hookean plus four fiber family strain energy function. Second, a thick-walled, bi-layered model was used to study changes in load bearing separately for the media and adventitia, with and without vasoconstriction. Third, a growth and remodeling approach was adopted to study our hypothesis that differences in contractility alone could differentiate between adaptive and maladaptive remodeling.

~~Additional methods are in **Supplemental Digital Content 1**, including those describing the quantitative histology, bulk RNA sequencing, immunohistochemistry, and biaxial biomechanical testing as well as novel computational modeling of biomechanical metrics useful for assessing local mechano-adaptations or the lack thereof.~~

Statistics. Data are presented as means±standard errors and analyzed using one- or two-way analysis of variance (ANOVA), as appropriate, with post-hoc Bonferroni tests; $p < 0.05$ was considered significant. Differential gene expression was determined by bulk RNA-sequencing and considered for multiple comparisons using the Benjamini-Hochberg method.

Results

Similar Baseline Material Composition, Properties, and Function Across Mouse Strains Suggest a Common Homeostatic State. Mechanical homeostasis within elastic arteries tends to maintain

circumferential wall stress and material stiffness near target values,[17] the latter of which reflects the underlying structural composition and organization of the arterial wall. Differences in baseline thoracic aortic composition were modest (non-significant) between age- and sex-matched normal adult C57BL/6J and 129S6/SvEvTac mice (**Supplemental Tables S1–S2** in **Supplemental Digital Content 1**), consistent with the modest differential gene expression (**Supplemental Figure S1** in **Supplemental Digital Content 1**). With regard to the primary load-bearing constituents, percentages of medial elastic fibers, smooth muscle cells, and fibrillar collagens were 36.5 vs. 39.5%, 38.4 vs. 40.1%, and 23.2 vs. 17.7% in the C57BL/6J and 129S6/SvEvTac aortas, respectively. The slightly higher (non-significant) medial collagen in the C57BL/6J aortas was offset by a slightly lower glycosaminoglycan amount; percentages of adventitial collagen fibers were nearly identical (~99.4%) in both strains.

Although the primary biological process associated with the differentially expressed genes at baseline was extracellular matrix organization (**Figure S1**), the biaxial biomechanical properties were yet similar statistically (**Table S3**; **Figure S2**; raw biomechanical data in **Supplemental Digital Content 2**). For example, baseline passive circumferential wall stress and material stiffness at comparable strain-specific systolic pressures (130 vs. 133 mmHg) were 311 vs. 301 kPa and 1.91 vs. 1.85 MPa for the C57BL/6J and 129S6/SvEvTac aortas, respectively. The overall baseline contractile capacity of the smooth muscle cells was also similar for the two strains (**Table S4**; **Figure S3**), with membrane depolarization via 100 mM KCl resulting in -19 and -23% reductions in outer-diameter and -38 and -43% reductions in circumferential wall stress in the C57BL/6J and 129S6/SvEvTac aortas, respectively; these measurements were at a common distension pressure of 90 mmHg and strain-specific values of axial stretch, which were also comparable (1.49 vs. 1.45). Similarities in these and other histo-mechanical metrics across these two strains support the existence of common homeostatic biomechanical set-points arising from similar baseline gene expression and microstructural features.

Distinct Hypertensive Remodeling Across Mouse Strains Results from Marked Differential Gene Expression. Mechano-adaptive arterial remodeling in hypertension requires the wall to thicken to offset the increase in blood pressure.[5] Whereas elevation of blood pressure following two weeks of AngII infusion was similar in both strains (baseline systolic pressures of 127 and 133 mmHg and hypertensive pressures of 167 and 175 mmHg for the C57BL/6J and 129S6/SvEvTac mice, respectively), wall thickening was very different. The hypertensive thoracic aorta thickened dramatically (~1.9-fold) in the C57BL/6J mice due to medial and especially adventitial thickening; by contrast, it thickened modestly (~1.13-fold) in the 129S6/SvEvTac mice (**Figure 1**). Of particular note was a dramatic increase in ~~mural collagen per~~ loaded cross-sectional collagen area in the C57BL/6J ~~mice~~adventitia~~,~~ (2.35-fold, $p = 0.004$), many fibers

of which were thicker than normal, and a trend towards a 1.75-fold increase in the media ($p = 0.078$; **Table S1**, which also quantifies the intima-media thickness, IMT)~~. with collagen fraction increasing 1.75-fold in the media ($p = 0.078$) and 2.35-fold in the adventitia ($p = 0.004$; **Table S1**, which also quantifies the intima-media thickness, IMT), many fibers of which were thicker than normal.~~ By contrast, percent medial and adventitial collagen fractions did not change significantly in the 129S6/SvEvTac aortas.

Bulk RNA sequencing (**Figures 2, S4**) confirmed marked increases in genes encoding structural proteins of the extracellular matrix in the hypertensive C57BL/6J mice, with significant increases in collagens *Col1a1*, *Col3a1*, and *Col5a1* as well as fibronectin *Fn1*, among others. Transcripts for matrix metalloproteinases *Mmp2*, *Mmp12*, and *Mmp13*, among others, were also increased. Full gene expression tables are in **Supplemental Digital Content 3**. Because these transcriptional changes were seen in both the C57BL/6J and 129S6/SvEvTac aortas, these data suggested marked matrix remodeling in both strains though with increased accumulation only in C57BL/6J. Despite modest expression differences in *Smad2*/*Smad3* (**Figure 2**), the TGF-beta signaling pathway expression was not significantly different between strains (MSigDB, p =0.24). Because it is difficult to distinguish newly synthesized or remodeled matrix from extant matrix, functional readouts such as those from careful biomechanical phenotyping become essential (see below).

Gene ontology studies revealed distinct primary biological processes for the fibrotic C57BL/6J and modestly adapted 129S6/SvEvTac aortas (**Figure 2**). Most notably, immune/inflammatory processes were significantly increased in the C57BL/6J aortas relative to the 129S6/SvEvTac aortas and, conversely, contractile processes were significantly increased in the 129S6/SvEvTac aortas relative to the C57BL/6J aortas. Similarly, Molecular Signatures Database (MSigDB) pathway-based analyses emphasized increased TNF-α signaling in C57BL/6J aortas and increased myogenesis in 129S6/SvEvTac aortas (**Figure S4**). Particularly increased was the gene for cytokine interleukin-6 (*Il6*) in the hypertensive C57BL/6J aortas (**Figure 2**). Immuno-staining confirmed a significant increase in inflammatory cells ($CD45^+$, a pan-leukocyte marker, and $CD68^+$, a macrophage marker) within the hypertensive C57BL/6J aortas, both in the media and especially in the adventitia where there was the most dramatic accumulation of collagen (**Figure 3; Tables S5–S6**). The number of immune cells was similar in the 129S6/SvEvTac aortas between baseline and hypertension. By contrast, ex vivo isobaric and axially isometric contraction studies revealed a significantly greater contractile response by the hypertensive 129S6/SvEvTac aortas in response to high KCl, phenylephrine (PE), and especially AngII as indicated by the active reduction in outer diameter (**Figure 3**). It is noted that increased smooth muscle contraction in vivo in response to the exogenous AngII would be expected to alter the pressure-distended state in which the extracellular matrix turned over.

Smooth Muscle Contractility is a Key Determinant of Wall Stress in Hypertensive Aortic Remodeling. Mean wall stress, and thus material stiffness, depend directly on the distending pressure as well as the luminal radius and wall thickness, the latter two of which depend on the nonlinear mechanical behavior of the wall and the contractile state. In particular, increased contractility reduces mean wall stress (σ_θ) by decreasing the luminal radius a and increasing the wall thickness h ($\sigma_\theta = Pa/h$ by Laplace's law where P is pressure).[18] Consistent with bulk RNAseq identification of upregulated contractile processes in the 129S6/SvEvTac aortas, ex vivo smooth muscle contraction in response to PE and AngII reduced wall stress dramatically (by 72 and 46%, respectively). By contrast, reductions in wall stress in response to PE and AngII were significantly less in the C57BL/6J aortas, 49 and 24%, respectively (**Table S4**, **Figure 3**). Importantly, the two-fold greater reduction in wall stress ex vivo in 129S6/SvEvTac than C57Bl/6J aortas in response to AngII suggests that the smooth muscle cells were better able to vasoconstrict the aorta in vivo in response to the exogenous AngII stimulus, thus reducing wall stress in vivo. Indeed, this difference in contractility to AngII also presented in the (normotensive) control groups (**Table S4**, **Figure 3**), suggesting that this difference was not a consequence of the chronic infusion of AngII.

These differences in smooth muscle cell contractile capacity between strains manifested despite similar overall increases in smooth muscle percentage within the media, which were 20.9% and 27.3% in the 129S6/SvEvTac and C57BL/6 aortas, respectively (**Table S1**). Taken together, these data are consistent with an increased contractile phenotype in the 129S6/SvEvTac and increased synthetic phenotype in the C57BL/6J aortas. Again, therefore, the need for functional readouts is clear as transcriptional and/or histological measurements alone are not sufficient to reveal tissue-level consequences.

Given that the histological, transcriptional, mechanical, and functional data consistently suggested the importance of inflammation in the fibrotic remodeling and contractility in the near adaptive remodeling, we used overall wall thickness as a metric of mechano-adaptation. There was a strong correlation between fibrotic thickening and $CD45^+$ cell staining and an even stronger inverse correlation between thickening and contractility (**Figure 3**, **Table S7**). Recalling our prior results in *Apoe*$^{-/-}$ mice wherein the thoracic aorta was fibrotic but the infrarenal aorta was not,[14] we tested the hypothesis that the adaptive capacity of the infrarenal aorta associated with a greater contractile capacity against AngII in those mice. New experiments confirmed this hypothesis, revealing that ex vivo vasoconstriction in response to exogenous AngII resulted in a 26.3% reduction in circumferential wall stress in the Apoe$^{-/-}$ infrarenal aorta but only a 3.9% reduction in the descending thoracic aorta (**Figure S5**). Indeed, vasoconstriction-based reductions in wall stress were similarly low in the ascending thoracic aorta (10.2%) and the suprarenal aorta (2.0%) in these mice, regions that also exhibited excessive wall thickening.[14]

Taken together, these findings are consistent with the hypothesis that modest hypertension-induced deviations in wall stress from the common homeostatic target value of wall stress lead to adaptive remodeling whereas large deviations in wall stress from normal can stimulate an inflammatory response and fibrotic remodeling.[14] That is, inflammation can be stimulated when normal mechanobiological responses are not sufficient, or rapid enough, to reduce perturbations to homeostasis.[1] Toward this end, recall that the greatest accumulation of collagen in hypertension was in the adventitia, the site of greatest $CD45^+$ cell staining. There is, therefore, a need to delineate changes in wall stress by layer.

Biomechanical Computations Suggest that Excessive Adventitial Wall Stress Drives Inflammation. The collagen-rich adventitia tends to serve as a protective sheath in elastic arteries, increasing its load carrying in cases of elevated blood pressure to protect the more vulnerable smooth muscle cells and elastic fibers of the medial layer.[19] Changes in wall stress have long been known to drive arterial remodeling.[4,5] Here we used three different, but related, methods to independently evaluate changes in wall stress across the four primary groups of mice, baseline and hypertensive C57BL/6J and 129S6/SvEvTac. First, we used the universal Laplace solution, which is independent of reference configuration and constitutive assumptions and always yields the correct mean value of wall stress (i.e., also in thick-walled vessels with transmural stress gradients). Because it is not possible to assess basal tone in conscious mice, we used the extremes of passive only and maximum contractile to bound the in vivo state. **Figure S6** shows that mean wall stress was restored to within its normal range in all but one of the six hypertensive 129S6/SvEvTac aortas when including smooth muscle contractility, but not in six of the seven hypertensive C57BL6J aortas. Indeed, wall stresses in four of the seven hypertensive C57BL/6J aortas were well below homeostatic target values, consistent with a maladaptive fibrotic response.

Findings from a bi-layered model of wall stress that accounts for the nonlinear material behaviors (**Figure 4**) suggested further that the adventitia tends initially to carry an increasing proportion of the pressure-induced load in hypertension, which is modulated by smooth muscle associated vasoconstriction (panels **A** vs. **B** and **C**). Importantly, the model also suggested that, because of the greater contractile response of the 129S6/SvEvTac than the C57BL/6J aorta to exogenous AngII both before and after two weeks of induced hypertension, the initial degree of increase in adventitial wall stress was greater in the C57BL/6J than that in the 129S6/SvEvTac aorta (panel **C**). Interestingly, the model suggested that the remodeling experienced by the 129S6/SvEvTac aorta over two weeks of hypertension was adaptive, preserving medial and especially adventitial wall stress within 15% of homeostatic (e.g., 220 vs. 194 kPa); by contrast, the remodeling experienced by the C57BL/6J aorta resulted in excessive wall thickening with adventitial wall stress falling well below its target value (panel **G**). These findings motivated the use of a

third model, which calculates the time course of changes in wall composition, properties, and function while delineating medial and adventitial remodeling via mechano- and immuno-mediated mechanisms (**Figures 5, S7**). This model also suggested that it was the increased inflammation-mediated thickening of the wall, especially in the adventitia where wall stress increased markedly, in the C57BL/6J aorta that drove the maladaptation while it was the contractile-mediated regelation of wall stress that enabled an adaptive remodeling in the 129S6/SvEvTac aorta.

Discussion

There are many reports of differences in vascular phenotype between 129S6/SvEvTac and C57BL/6J mice. Capillary density increases more quickly in Sv129 than in C57BL/6 mice following hind-limb ischemia;[20] mutations to the gene that encodes fibrillin-1 (*Fbn1*) and causes Marfan syndrome result in an earlier disease presentation in 129/Sv than in C57BL/6 mice;[21] mechanical consequences of elastin haploinsufficiency are greater in C57BL/6J;*Eln*$^{+/-}$x129X1/SvJ mice than in C57BL/6J;*Eln*$^{+/-}$ mice;[22] and the atherosclerotic burden in the aortic arch of *Apoe*$^{-/-}$ mice is greater on a 129S6 than C57BL/6J background[23] (further discussion in **Supplemental Digital Content 1**). Interestingly, it was recently suggested that it is two key modifier genes (*Map2k6* and *Mmp17*) that increase aortopathy in Marfan Syndrome in 129S6 relative to C57BL/6J mice.[24] We confirmed that both of these genes are expressed at higher levels in 129S6/SvEvTac than in C57BL/6J aortas. Although *Map2k6* (encoding MEK6) is upstream of p38 MAPK, which has been implicated in the fibrotic response in C57BL/6J mice,[9,10] and *Mmp17* (encoding MT4-MMP) is involved in activating inflammatory mediators that include TNF-α (recall **Table S4**), these two genes were not in the top 100 differentially expressed genes herein and they did not differ significantly between strains following AngII infusion. Thus, we focused primarily on functional readouts, with the present findings demonstrating that many baseline compositional, mechanical, and functional metrics for the thoracic aorta are similar between these two strains consistent with common mechanical homeostatic set-points. Although both circumferential wall stress and material stiffness are highly mechano-regulated in large arteries,[6,17] we focused on wall stress despite quantifying multiple biomechanical metrics.

The renin-angiotensin system plays a central role in many cases of hypertension, hence chronic infusion of AngII in mice is a well-accepted and widely-used model.[25] Notwithstanding its clinical relevance, interpretations of arterial remodeling in AngII-infusion studies can be complicated by the myriad effects of this peptide. AngII increases blood pressure, which increases mechanical stress in the wall, but it is also pro-inflammatory. Cell culture, ex vivo perfusion, and in vivo (e.g., aortic banding) studies all show that increased mechanical stress/stretch drives differential gene expression in medial

smooth muscle cells and adventitial fibroblasts, often leading to increased extracellular matrix turnover, namely, synthesis of matrix proteins and matrix degrading enzymes.[8,9,26-29] Conversely, cell culture and ex vivo perfusion studies show that AngII alone can similarly drive matrix turnover, again via both increased matrix and matrix degrading enzymes.[9,26,28,30,31] AngII also directly induces production of monocyte chemoattractant protein-1 (MCP-1) and IL-6, both of which drive inflammation.[32,33] In all of these cases, these effects of AngII are through the AT_1 receptor (AT_{1a} in mice in most cases except contractility, which is driven by AT_{1b}).[34]

Importantly, the density of AT_1 receptors increases from the thoracic aorta to the infrarenal abdominal aorta,[34] hence one cannot explain the aforementioned fibrosis of the thoracic aorta or its absence in the infrarenal aorta in AngII-infused *Apoe*$^{-/-}$ mice on a C57BL/6 background[14] based solely on the pro-inflammatory actions of AngII via AT_1R. Noting that the density of the AT_{1b} receptor is ~3-fold higher than that of the AT_{1a} in all regions[34] supports, however, the hypothesis that increased vasoconstriction in the infrarenal aorta against exogenous AngII may be protective by reducing wall stress (**Figure S5**). Our RNAseq data revealed that AT_{1a} transcripts were elevated in the C57BL/6J relative to the 129S6/SvEvTac thoracic aortas, but not significantly (**Figure 2**). Hence, it does not appear that the pro-inflammatory action of AngII acting locally via AT_{1a} alone was responsible for the marked fibrosis in the former but not the latter. Transcripts for collagens (*Col1a1*, *Col3a1*, *Col5a1*) were increased in hypertensive aortas from both C57BL/6J and 129S6/SvEvTac mice, though more so in the C57BL/6J aortas consistent with the marked fibrosis therein and a prior report[9,10]. Transcripts for MMP-2 and -13 were also higher in the C57BL/6J aortas, emphasizing that it was turnover of matrix with increased accumulation in the fibrotic case. Markers of cell proliferation (*Pcna*) and apoptosis (*Casp3*) were similarly higher in the C57BL/6J aortas, again consistent with an increased turnover (**Figures 2 and S8**). There were surprisingly few significant differences in integrin transcripts between the two strains, though transcripts for α_5 and β_1 increased more in the 129S6/SvEvTac aortas. Most importantly, however, consistent with the gene ontology studies indicating greater immune processes in the C57BL/6J and greater contractile processes in the 129S6/SvEvTac aortas, the transcript for IL-6 (*Il6*) was markedly higher, consistent with prior studies,[35] and those for smooth muscle myosin heavy chain and alpha actin (*Myh11* and *Acta2*) were markedly lower in the C57BL/6 aortas (**Figure 2**). Notably, the amount of medial smooth muscle tissue staining (greater in C57BL/6 AngII than 129S6/SvEvTac AngII aortas; **Table S1**) does not explain the observed strain difference in contraction. That is, differences in smooth muscle phenotype, not percentage, were likely responsible for the contractility difference.

Given consistent results of the three independent biomechanical models of wall stress (**Figures 4, 5, S6, S7**), it appears that the increased contractility against the exogenous AngII in the 129S6/SvEvTac aortas reduced pressure-induced wall stress significantly, especially in the adventitia, thus allowing modest wall thickening to restore the modestly perturbed wall stresses back towards homeostatic. By contrast, it appears that the excessive wall stress in the C57BL/6J aortas, especially in the adventitia, contributed to the recruitment of inflammatory cells to the adventitia (**Figures 3 and S3, Tables S5–S6**) to help lower wall stress by stimulating further production of matrix; such production was excessive, however, resulting in a fibrotic adventitia (**Figure 1**) reflective of lost homeostasis. A protective role of increased smooth muscle contractility is supported further by prior experiments that revealed that the degree of adventitial fibrosis in the thoracic aorta of AngII-infused C57BL/6 mice correlates directly with diminished vasoconstrictive strength.[16] Interestingly, aortic remodeling is also modest-to-moderate in all regions in norepinephrine-induced hypertension,[36] noting that these regions are highly vasoconstrictive to phenylephrine ex vivo in mice on a C57BL/6 background (**Figure S5**). Other in vivo studies that support the importance of the degree of wall stress in dictating the degree of adventitial remodeling include an integrin knockout model and the use of an anti-hypertensive drug to reduce the pressure-induced wall stress, both in C57BL/6 mice. The former showed that disruption of the α_1-integrin subunit (which binds collagen) did not affect blood pressure in AngII-infused mice, but nevertheless blunted carotid artery (especially adventitial) remodeling,[36] suggesting that it is the value of the sensed stress that stimulates the remodeling response. The latter showed that hydralazine reduces the blood pressure elevation in AngII-infused mice (despite persistence of a pro-inflammatory peptide), which in turn reduced the accumulation of adventitial collagen.[9] Hence, whether the sensed wall stress was reduced by increased contractility, integrin disruption, or pressure reduction, in each case the degree of collagen accumulation was reduced significantly.

That increased wall stress, particularly in the adventitia, precedes the inflammation-driven accumulation of matrix is consistent with the timing observed previously in AngII-infused *Apoe*$^{-/-}$ mice (Figures 3–4 in Ref. 14), and consistent with the concept that inflammation can promote or prevent tissue homeostasis, namely, that inflammation can be engaged when normal homeostatic mechanisms are either not sufficient or rapid enough to resolve the perturbation; large perturbations can lead, however, to marked inflammation that prevents homeostasis.[1] The present study highlights the role of smooth muscle contractility in modulating this wall stress. Toward this end, it is important to rethink of the Laplace equation as $\sigma_\theta = Pa(P,C)/h(P,C)$, where P is pressure and C is contractility, with luminal radius a governed by both P and C (i.e., $a = a(P,C)$) and similarly for wall thickness ($h = h(P,C)$). Pressure-

induced increases in radius and decreases in thickness (isochorically) can thus be offset by contraction-induced decreases in radius and increases in thickness, thus decreasing the degree of perturbation of wall stress from its homeostatic target.

There is, of course, a need to study in more detail both the time-course of pressure elevation and associated remodeling in other elastic and muscular arteries. We only studied the thoracic aorta after two weeks of AngII-induced hypertension in each model, thus we do not know whether the remodeling might have become maladaptive at longer times in the 129S6/SvEvTac mice. We have shown previously, however, that AngII-induced hypertensive remodeling in C57BL/6 aortas tends not to differ over two-to-four weeks of infusion[15,16] and that hypertension induced in C57BL/6;129S6 mice over longer periods (13 to 18 weeks) by a high salt diet plus L-NAME did not cause adverse fibrotic remodeling in these vessels.[13,37] Interestingly, large (elastic) arteries tend to remodel more in response to hypertension and aging than do medium-sized (muscular) arteries,[38] which have greater contractile responsiveness.[39] Comparisons of the time-course of remodeling of arteries within different locations within the same mouse models would thus be expected to be informative. There is also a need to consider other models of induced hypertension and a need to study mice having other genetic backgrounds. Prior findings in mixed C57BL/6;129S6 mice, which also have similar baseline compositions and properties, were similar to the present findings for the 129S6/SvEvTac mice when infused with AngII (**Tables S8–S9**). Finally, we note that rates of hypertensive remodeling may differ between species. E.g., in rabbits, it takes approximately two months for vascular adaption to hypertension to occur[40] and for rats likely more than a month.[41]

In conclusion, we acknowledge the extreme biological complexity of hypertensive remodeling of the aorta and that different genetic backgrounds further complicate the interpretation of data. Nevertheless, histological, transcriptional, mechanical, functional, and computational findings herein all suggest a detrimental role of excessive mechanical stress-mediated inflammation in promoting aortic fibrosis in (AngII-infused C57BL/6J mice) hypertension and conversely a protective role of enhanced smooth muscle contractility in reducing wall stress and thereby promoting mechanical homeostasis without the need to invoke inflammatory support, which can otherwise prevent rather than promote homeostasis depending on the perturbation in hemodynamic loading.

Perspectives

- Baseline aortic composition, mechanical properties, and vasoconstrictive capacity are similar in C57BL/6 and 129S6 aortas, suggesting common homeostatic biomechanical targets;

- Aortic remodeling in response to chronic angiotensin II-induced hypertension differs dramatically between C57BL/6 and 129S6 mice, with gross collagen accumulation and over-thickening of the wall in the former and modest thickening in the latter;
- RNA sequencing-based gene ontologies show increased immune/inflammatory processes in C57BL/6 but increased contractile processes in 129S6 mice, confirmed by histology and ex vivo contraction studies. Fibrotic thickening correlated positively with increased inflammation and negatively with increased contractility;
- Three independent computational biomechanical models suggest that increased contractile-mediated reductions in wall stress facilitate adaptive hypertensive remodeling, negating the need for subsequent inflammation that can drive fibrosis, especially in the adventitia.

Sources of Funding

This work was supported by grants from NIH (R01-HL105297, P01-HL134605, U01-HL142518, R01-HL146723), Netherlands Organisation for Scientific Research (Rubicon 452172006), and the European Union's Horizon 2020 research and innovation program (No 793805).

Author Contributions

BS: conceptualization, data curation, formal analysis, funding acquisition, investigation, methodology, project administration, software, supervision, visualization, writing – original draft, writing – review & editing; ML: formal analysis, methodology, software, validation, visualization, writing – original draft, writing – review & editing; MW: investigation, methodology, resources; SM: data curation, formal analysis, investigation, resources; AWC: investigation, methodology, validation, writing – review & editing; PR: investigation, methodology; ABR: investigation, methodology; S-IM: investigation, methodology, writing – review & editing; AR: investigation, writing – review & editing; C-SH: investigation, methodology; BJ: investigation, methodology; MRB: data curation, formal analysis, investigation, writing – review & editing; GT: methodology, resources, supervision, writing – review & editing; JDH: conceptualization, funding acquisition, project administration, resources, supervision, writing – original draft, writing – review & editing.

Disclosures

None.

References

1. Chovatiya R, Medzhitov R. Stress, inflammation, and defense of homeostasis. *Mol Cell*. 2014;54:281-288.
2. Tzima E, Irani-Tehrani M, Kiosses WB, Dejana E, Schultz DA, Engelhardt B, Cao G, DeLisser H, Schwartz MA. A mechanosensory complex that mediates the endothelial cell response to fluid shear stress. *Nature*. 2005;437:426-431.
3. Chien S. Mechanotransduction and endothelial cell homeostasis: The wisdom of the cell. *Am J Physiol Heart Circ Physiol*. 2007;292:H1209-1224.
4. Dajnowiec D, Langille BL. Arterial adaptations to chronic changes in haemodynamic function: Coupling vasomotor tone to structural remodelling. *Clin Sci (Lond)*. 2007;113:15-23.
5. Hayashi K, Naiki T. Adaptation and remodeling of vascular wall; biomechanical response to hypertension. *J Mech Behav Biomed Mater*. 2009;2:3-19.
6. Humphrey JD. Mechanisms of arterial remodeling in hypertension: Coupled roles of wall shear and intramural stress. *Hypertension*. 2008;52:195-200.
7. Guzik TJ, Hoch NE, Brown KA, McCann LA, Rahman A, Dikalov S, Goronzy J, Weyand C, Harrison DG. Role of the t cell in the genesis of angiotensin ii induced hypertension and vascular dysfunction. *J Exp Med*. 2007;204:2449-2460.
8. Kuang SQ, Geng L, Prakash SK, Cao JM, Guo S, Villamizar C, Kwartler CS, Peters AM, Brasier AR, Milewicz DM. Aortic remodeling after transverse aortic constriction in mice is attenuated with at1 receptor blockade. *Arterioscler Thromb Vasc Biol*. 2013;33:2172-2179.
9. Wu J, Thabet SR, Kirabo A, Trott DW, Saleh MA, Xiao L, Madhur MS, Chen W, Harrison DG. Inflammation and mechanical stretch promote aortic stiffening in hypertension through activation of p38 mitogen-activated protein kinase. *Circ Res*. 2014;114:616-625.
10. Moore JP, Vinh A, Tuck KL, Sakkal S, Krishnan SM, Chan CT, Lieu M, Samuel CS, Diep H, Kemp-Harper BK, Tare M, Ricardo SD, Guzik TJ, Sobey CG, Drummond GR. M2 macrophage accumulation in the aortic wall during angiotensin ii infusion in mice is associated with fibrosis, elastin loss, and elevated blood pressure. *Am J Physiol Heart Circ Physiol*. 2015;309:H906-917.
11. Tang PC, Qin L, Zielonka J, Zhou J, Matte-Martone C, Bergaya S, van Rooijen N, Shlomchik WD, Min W, Sessa WC, Pober JS, Tellides G. Myd88-dependent, superoxide-initiated inflammation is necessary for flow-mediated inward remodeling of conduit arteries. *J Exp Med*. 2008;205:3159-3171.

12. Zhou J, Tang PC, Qin L, Gayed PM, Li W, Skokos EA, Kyriakides TR, Pober JS, Tellides G. Cxcr3-dependent accumulation and activation of perivascular macrophages is necessary for homeostatic arterial remodeling to hemodynamic stresses. *J Exp Med*. 2010;207:1951-1966.
13. Spronck B, Ferruzzi J, Bellini C, Caulk AW, Murtada S-I, Humphrey JD. Aortic remodeling is modest and sex-independent in mice when hypertension is superimposed on aging. *J Hypertens*. 2020;38:1312-1321.
14. Bersi MR, Khosravi R, Wujciak AJ, Harrison DG, Humphrey JD. Differential cell-matrix mechanoadaptations and inflammation drive regional propensities to aortic fibrosis, aneurysm or dissection in hypertension. *J R Soc Interface*. 2017;14:20170327.
15. Bersi MR, Bellini C, Wu J, Montaniel KRC, Harrison DG, Humphrey JD. Excessive adventitial remodeling leads to early aortic maladaptation in angiotensin-induced hypertension. *Hypertension*. 2016;67:890-896.
16. Korneva A, Humphrey JD. Maladaptive aortic remodeling in hypertension associates with dysfunctional smooth muscle contractility. *Am J Physiol Heart Circ Physiol*. 2019;316:H265-H278.
17. Wagenseil JE, Mecham RP. Vascular extracellular matrix and arterial mechanics. *Physiol Rev*. 2009;89:957-989.
18. Humphrey JD. Mechanisms of vascular remodeling in hypertension. *Am J Hypertens*. 2020
19. Bellini C, Ferruzzi J, Roccabianca S, Di Martino ES, Humphrey JD. A microstructurally motivated model of arterial wall mechanics with mechanobiological implications. *Ann Biomed Eng*. 2014;42:488-502.
20. Scholz D, Ziegelhoeffer T, Helisch A, Wagner S, Friedrich C, Podzuweit T, Schaper W. Contribution of arteriogenesis and angiogenesis to postocclusive hindlimb perfusion in mice. *J Mol Cell Cardiol*. 2002;34:775-787.
21. Lima BL, Santos EJ, Fernandes GR, Merkel C, Mello MR, Gomes JP, Soukoyan M, Kerkis A, Massironi SM, Visintin JA, Pereira LV. A new mouse model for marfan syndrome presents phenotypic variability associated with the genetic background and overall levels of fbn1 expression. *PLoS One*. 2010;5:e14136.
22. Kozel BA, Knutsen RH, Ye L, Ciliberto CH, Broekelmann TJ, Mecham RP. Genetic modifiers of cardiovascular phenotype caused by elastin haploinsufficiency act by extrinsic noncomplementation. *J Biol Chem*. 2011;286:44926-44936.

23. Tomita H, Hagaman J, Friedman MH, Maeda N. Relationship between hemodynamics and atherosclerosis in aortic arches of apolipoprotein e-null mice on 129s6/svevtac and c57bl/6j genetic backgrounds. *Atherosclerosis*. 2012;220:78-85.
24. Doyle JJ, Doyle AJ, Wardlow RD, Bedja D, Dietz HC. Letting nature teach us how to cure genetic disease: The identification of modifier genes. *Journal of American Association for Pediatric Ophthalmology and Strabismus {JAAPOS}*. 2018;22:e27.
25. Lerman LO, Kurtz TW, Touyz RM, Ellison DH, Chade AR, Crowley SD, Mattson DL, Mullins JJ, Osborn J, Eirin A, Reckelhoff JF, Iadecola C, Coffman TM. Animal models of hypertension: A scientific statement from the american heart association. *Hypertension*. 2019;73:e87-e120.
26. Bardy N, Merval R, Benessiano J, Samuel JL, Tedgui A. Pressure and angiotensin ii synergistically induce aortic fibronectin expression in organ culture model of rabbit aorta. Evidence for a pressure-induced tissue renin-angiotensin system. *Circ Res*. 1996;79:70-78.
27. Ruddy JM, Jones JA, Stroud RE, Mukherjee R, Spinale FG, Ikonomidis JS. Differential effects of mechanical and biological stimuli on matrix metalloproteinase promoter activation in the thoracic aorta. *Circulation*. 2009;120:S262-268.
28. Stanley AG, Patel H, Knight AL, Williams B. Mechanical strain-induced human vascular matrix synthesis: The role of angiotensin ii. *J Renin Angiotensin Aldosterone Syst*. 2000;1:32-35.
29. Li Q, Muragaki Y, Hatamura I, Ueno H, Ooshima A. Stretch-induced collagen synthesis in cultured smooth muscle cells from rabbit aortic media and a possible involvement of angiotensin ii and transforming growth factor-beta. *J Vasc Res*. 1998;35:93-103.
30. Ford CM, Li S, Pickering JG. Angiotensin ii stimulates collagen synthesis in human vascular smooth muscle cells. Involvement of the at(1) receptor, transforming growth factor-beta, and tyrosine phosphorylation. *Arterioscler Thromb Vasc Biol*. 1999;19:1843-1851.
31. Tieu BC, Ju X, Lee C, Sun H, Lejeune W, Recinos A, 3rd, Brasier AR, Tilton RG. Aortic adventitial fibroblasts participate in angiotensin-induced vascular wall inflammation and remodeling. *J Vasc Res*. 2011;48:261-272.
32. Han Y, Runge MS, Brasier AR. Angiotensin ii induces interleukin-6 transcription in vascular smooth muscle cells through pleiotropic activation of nuclear factor-kappa b transcription factors. *Circ Res*. 1999;84:695-703.
33. Ishibashi M, Hiasa K, Zhao Q, Inoue S, Ohtani K, Kitamoto S, Tsuchihashi M, Sugaya T, Charo IF, Kura S, Tsuzuki T, Ishibashi T, Takeshita A, Egashira K. Critical role of monocyte chemoattractant

protein-1 receptor ccr2 on monocytes in hypertension-induced vascular inflammation and remodeling. *Circ Res*. 2004;94:1203-1210.

34. Poduri A, Owens AP, 3rd, Howatt DA, Moorleghen JJ, Balakrishnan A, Cassis LA, Daugherty A. Regional variation in aortic at1b receptor mrna abundance is associated with contractility but unrelated to atherosclerosis and aortic aneurysms. *PLoS One*. 2012;7:e48462.
35. Schrader LI, Kinzenbaw DA, Johnson AW, Faraci FM, Didion SP. Il-6 deficiency protects against angiotensin ii induced endothelial dysfunction and hypertrophy. *Arterioscler Thromb Vasc Biol*. 2007;27:2576-2581.
36. Louis H, Kakou A, Regnault V, Labat C, Bressenot A, Gao-Li J, Gardner H, Thornton SN, Challande P, Li Z, Lacolley P. Role of alpha1beta1-integrin in arterial stiffness and angiotensin-induced arterial wall hypertrophy in mice. *Am J Physiol Heart Circ Physiol*. 2007;293:H2597-H2604.
37. Bellini C, Wang S, Milewicz DM, Humphrey JD. Myh11(r247c/r247c) mutations increase thoracic aorta vulnerability to intramural damage despite a general biomechanical adaptivity. *J Biomech*. 2015;48:113-121.
38. Laurent S, Boutouyrie P. The structural factor of hypertension: Large and small artery alterations. *Circ Res*. 2015;116:1007-1021.
39. Murtada S-I, Kawamura Y, Weiss D, Humphrey JD. Differential biomechanical responses of elastic and muscular arteries to angiotensin ii-induced hypertension. *J Biomech*. 2021;[accepted]
40. Brownlee RD, Langille BL. Arterial adaptations to altered blood flow. *Can J Physiol Pharmacol*. 1991;69:978-983.
41. Fung YC, Liu SQ. Change of residual strains in arteries due to hypertrophy caused by aortic constriction. *Circ Res*. 1989;65:1340-1349.

Novelty and Significance

What is New?

- Maladaptive aortic remodeling associates with marked initial increases in wall stress and subsequent inflammation;
- Preserved cell contractility maintains wall stress near normal and prevents inflammation-driven maladaptation.

What is Relevant?

- Treatment of hypertension should lower blood pressure while maintaining vascular tone in proximal arteries to minimize their inflammatory response and thus stiffening;
- Hypertension studies in mice should carefully consider genetic background. Caution is warranted when comparing angiotensin II-infusion studies in different strains.

Summary

Excessive adventitial wall stress drives inflammation-mediated fibrosis in hypertensive aortic remodeling in C57BL/6 mice. Contraction-normalized adventitial wall stress in 129S6 mice prevents such fibrosis.

Figures

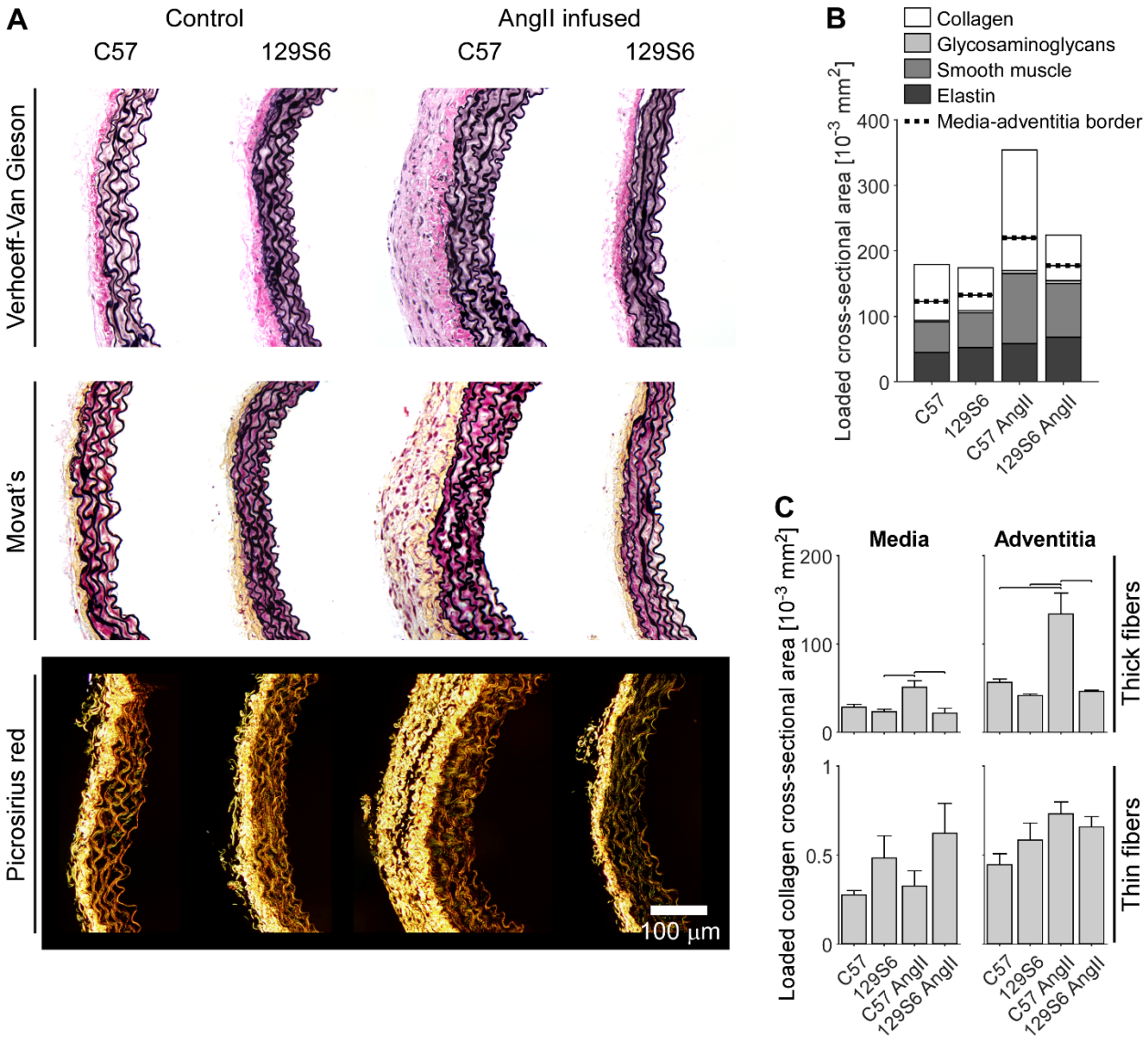

Figure 1. Chronic AngII-infusion causes marked medial and adventitial thickening in thoracic aortas from C57BL/6J, but not 129S6/SvEvTac, mice. **A**: Representative histological sections. **B**: Cross-sectional area of four major wall constituents for media (below dotted line) and adventitia (above dotted line); quantification in **Table S1**. **C**: Collagen content stratified to thick (red/orange, **Table S2**) and thin (yellow/green, **Table S2**) fibers. Bars denote statistically significant differences (p<0.05, two-way ANOVA with post-hoc Bonferroni test).

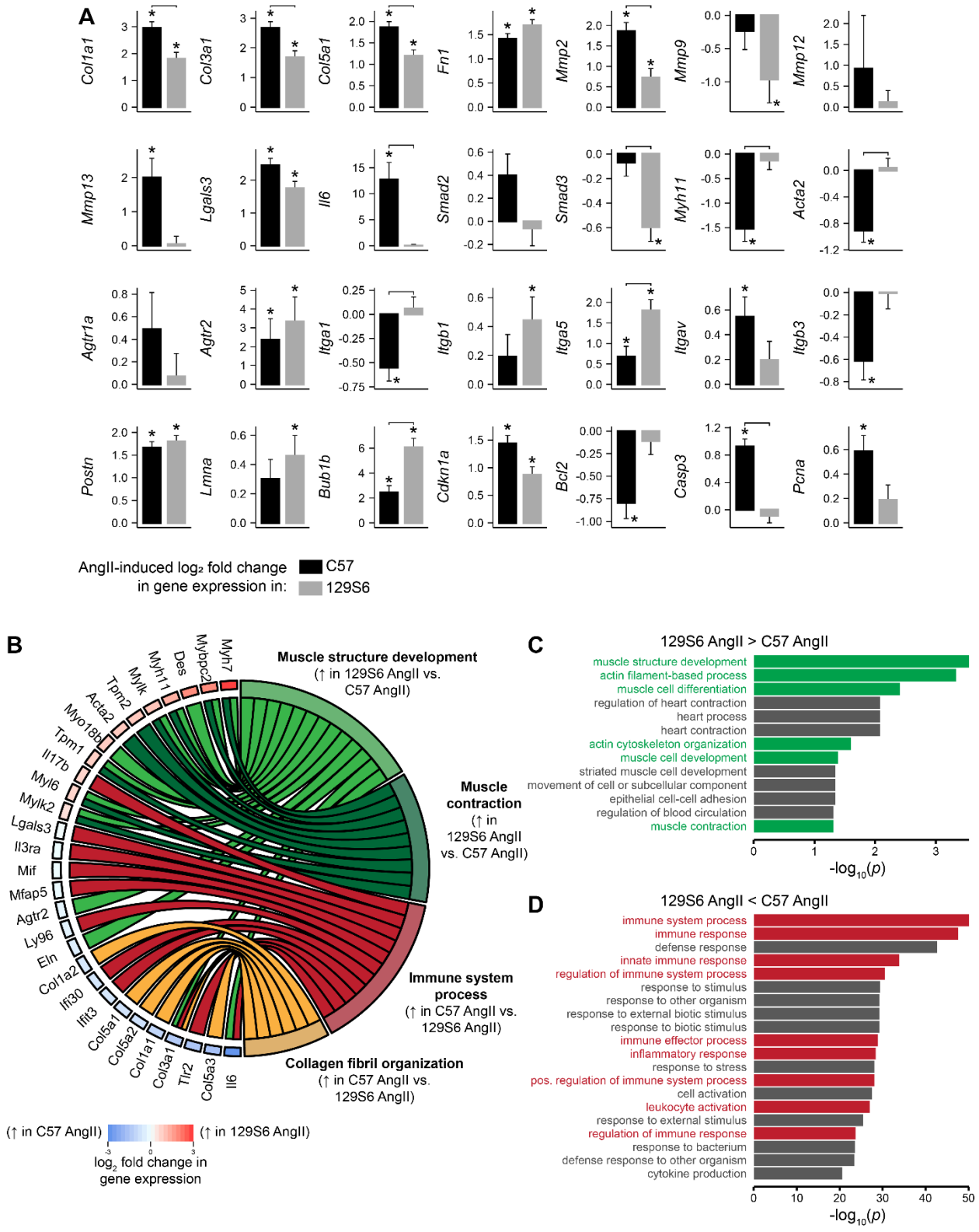

Figure 2. A: AngII-induced differential gene expression (after vs. before infusion) quantified by bulk RNA sequencing. Note, in particular, the upregulation of matrix and inflammatory markers and downregulation of contractile markers in the AngII-induced hypertensive C57BL/6J aortas. *p<0.05 for differential gene

expression. Horizontal brackets indicate significant (p<0.05) differences between the differential gene expressions of the two strains (interaction effect). AngII, angiotensin II infusion. **B–D**: Gene ontology (GO) analyses revealed that biological processes associated with immune processes and inflammation were significantly upregulated in AngII-infused C57BL/6 aortas relative to 129S6/SvEvTac aortas whereas muscle and its contraction were significantly upregulated in AngII-infused 129S6/SvEvTac aortas relative to C57BL/6 aortas.

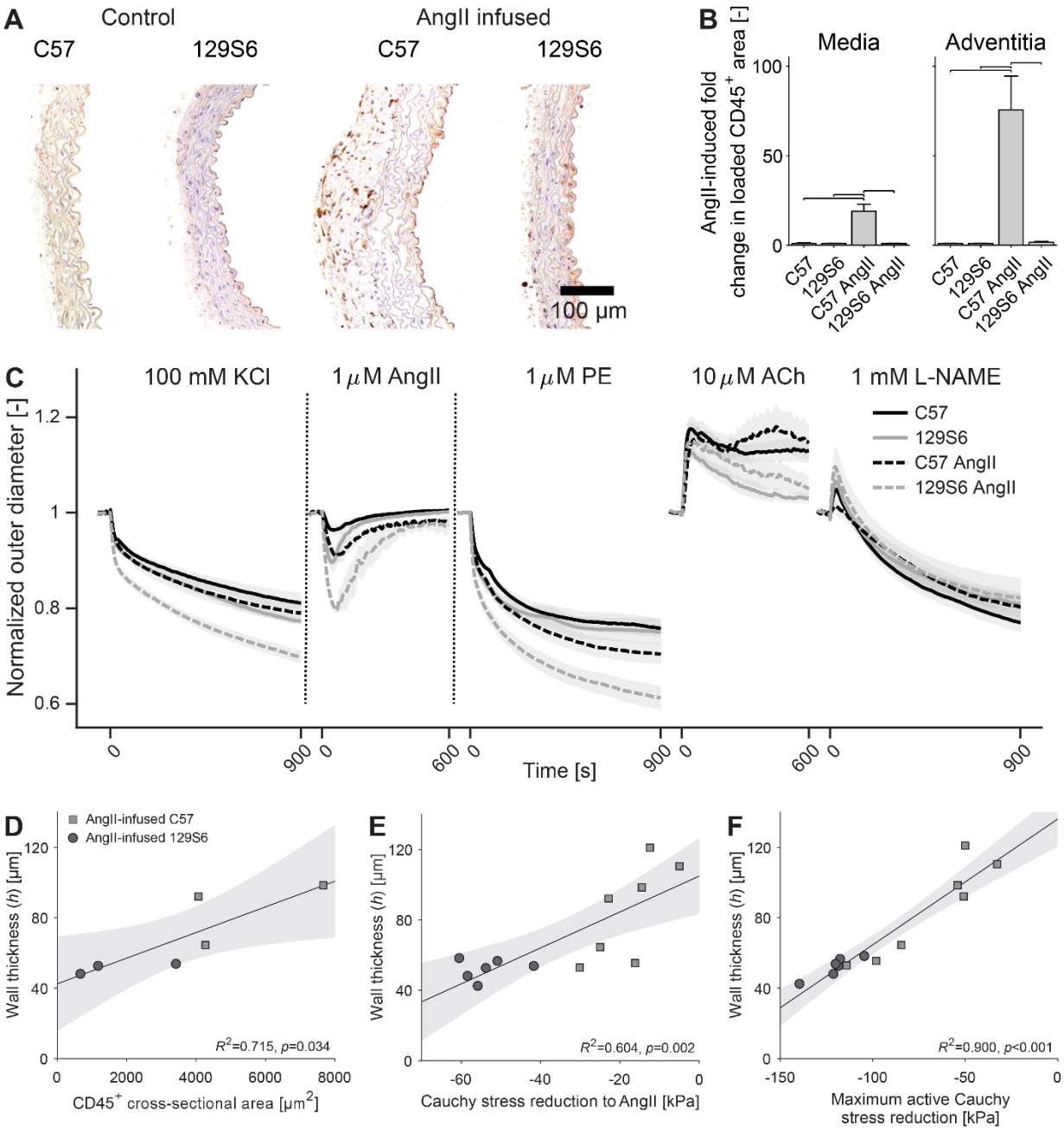

Figure 3. **A**: Representative CD45 immunohistochemistry. **B**: Normalized loaded CD45$^+$ cell cross-sectional area. Bars denote statistically significant differences (p<0.05, two-way ANOVA with post-hoc Bonferroni test); quantification in **Table S5**. **C**: Thoracic aortas from 129S6/SvEvTac mice show greater vasoconstriction to potassium chloride (KCl), angiotensin II (AngII), and phenylephrine (PE) than those from C57BL/6J mice and this difference increased after AngII-induced hypertension; in contrast, endothelial-dependent vasodilatation is affected modestly by hypertension in both strains. Plots show normalized outer diameter as a function of time during ex vivo vasoactive testing for all four groups. Lines indicate mean values; shaded areas indicate the standard error. Vertical dotted lines indicate 600-second washout steps. Actual outer diameter responses are in **Figure S3**; values and statistics are in **Table S4**. ACh, acetylcholine; L-NAME, N_ω-nitro-L-arginine methyl ester. **D–F:** Hypertension-induced changes in wall

thickness correlate positively with $CD45^+$ cell presence (**D**), but strongly and negatively with the ability of the smooth muscle to contract to AngII and other stimulants (**E,F**). Statistical comparison (**Table S7**) identified contractility as the stronger predictor of wall thickness/remodeling. Lines represent linear regressions, with 95%-confidence intervals shown with grey shading. Wall thicknesses were evaluated at a common pressure of 100 mmHg but individual axial stretches.

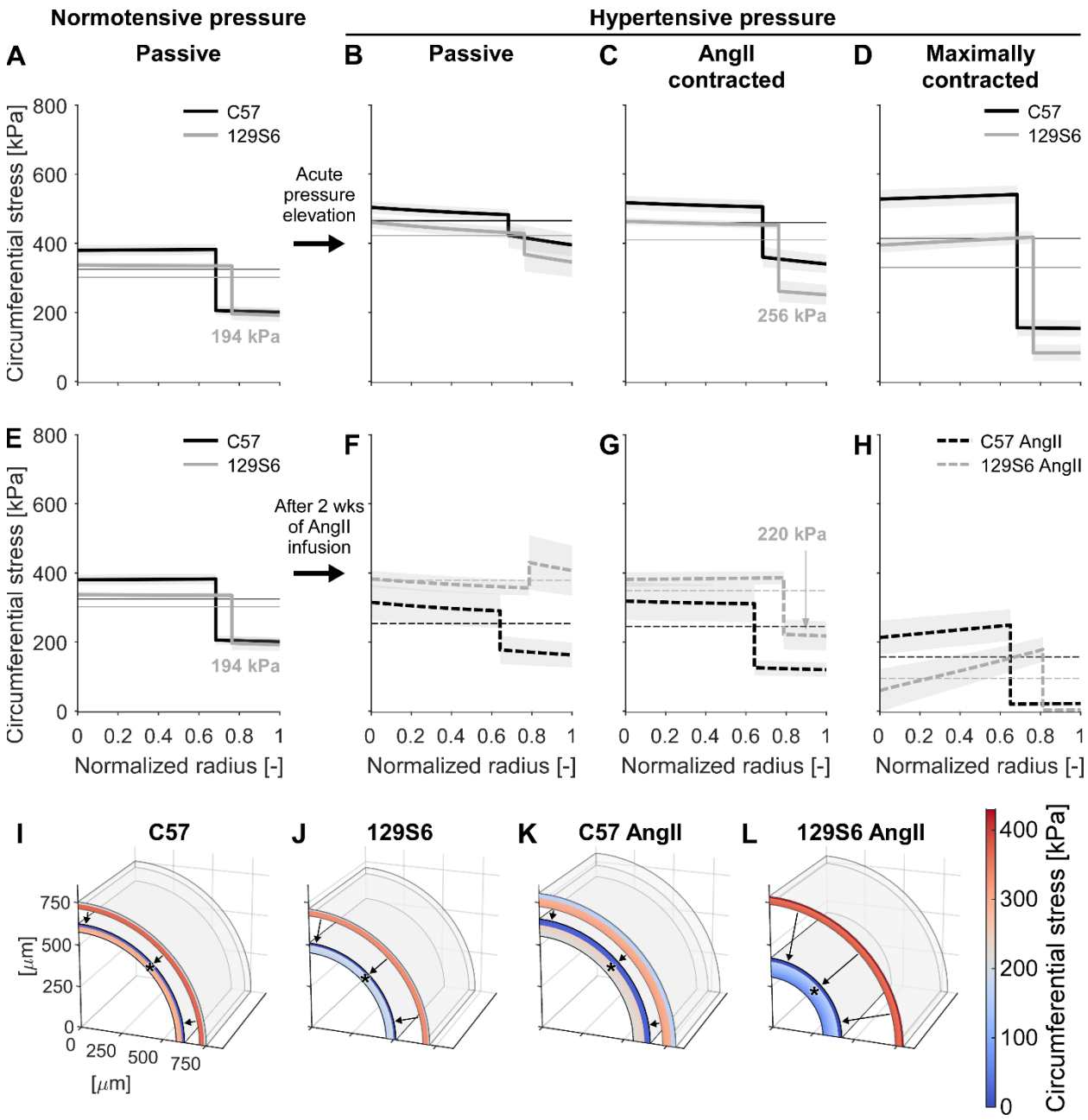

Figure 4. A–H: Calculated transmural distributions of circumferential Cauchy wall stress. Thin, horizontal lines represent the circumferential stress calculated using Laplace's law ~~(model 1)~~. (**A,E**) The media carries most of the circumferential wall stress under normotensive conditions ~~(model 2)~~, as appropriate for storing elastic energy during systole that can be used during diastole to work on the distending fluid. (**B**) A simulated acute increase in blood pressure causes more load to be borne by the adventitia, (**C**) which can be reversed through vasoconstriction to angiotensin II (AngII). Panel **D** shows the vessel in a maximally contracted state (phenylephrine + L-NAME) to provide an upper-bound reference behavior. Even when maximally contracted, in contrast to the 129S6/SvEvTac aorta, the C57BL/6J aorta is unable to reduce its overall (Laplace) stress towards the normotensive value. (**F**) If only considering passive mechanical properties, AngII-induced hypertension and remodeling would cause adventitial load bearing to surpass medial load bearing in 129S6/SvEvTac but not in C57BL/6J aortas, yet (**G,H**) the 129S6/SvEvTac aorta is able to negate this *in vivo* through vasoconstriction. These simulations support the correlative finding of

Figure 3 that increased smooth muscle contraction plays a key role in the appropriate remodeling of the aorta in the 129S6/SvEvTac mice. Shaded areas indicate the standard error. Panel **E** replicates panel **A**, for easy comparison to panels **F–H**. Panels **I–L** illustrate the large effect of maximum contraction (* denotes contracted state; arrows indicate contraction) on geometry and stress; see the **Video** in **Supplemental Digital Content 4**.

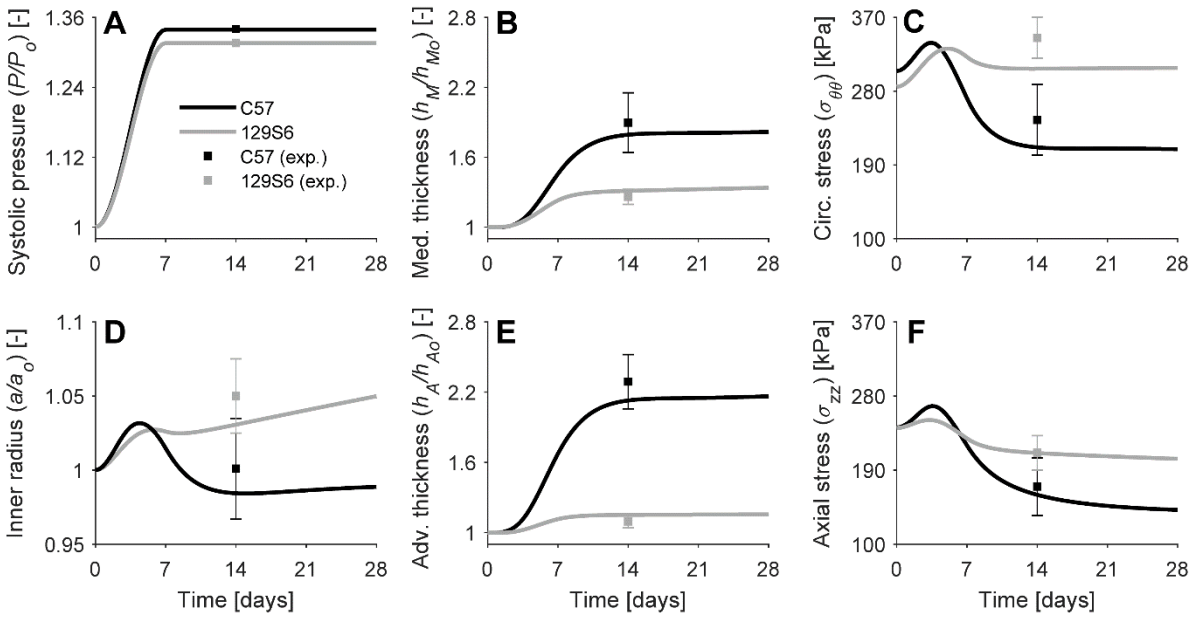

Figure 5. Computational growth & remodeling predictions (model 3) of responses following early, then sustained 1.34- or 1.32-fold increases in systolic pressure (**A**, model input): medial (med., **B**) and adventitial (adv., **E**) thickness (with quantities normalized to values at time 0 prior to AngII infusion) as well as (**D**) luminal radius and mean circumferential (circ., **C**) and axial (**F**) stress for the C57BL/6J (black) and 129S6/SvEvTac (grey) mice. Simulations are shown for a simultaneous increase in smooth muscle tone from day 0 (passive behavior) to respective AngII-appropriate levels under hypertensive conditions at day 7, then preserved. Stress-mediated inflammatory effects are computed internally by the model, resulting in a marked inflammatory response for the C57BL/6J but not the 129S6/SvEvTac aorta (**Figure S7L**). Shown, too, are means±standard errors of experimental values (squares with whiskers), noting that the model was informed by pre-hypertensive values, hence the simulations are predictions, not descriptions, of measured quantities. Note the dramatic increase in adventitial and medial thickness for the C57BL/6J aorta, and associated decrease in stress, by day 14, consistent with a delayed but exuberant production of inflammatory collagen primarily within the adventitia (**Figure S7G**).